



**HAL**  
open science

## Water oxidation with inhomogeneous metal-silicon interfaces

Gabriel Loget

► **To cite this version:**

Gabriel Loget. Water oxidation with inhomogeneous metal-silicon interfaces. *Current Opinion in Colloid & Interface Science*, 2019, 39, pp.40-50. 10.1016/j.cocis.2019.01.001 . hal-02991335

**HAL Id: hal-02991335**

**<https://hal.science/hal-02991335>**

Submitted on 5 Nov 2020

**HAL** is a multi-disciplinary open access archive for the deposit and dissemination of scientific research documents, whether they are published or not. The documents may come from teaching and research institutions in France or abroad, or from public or private research centers.

L'archive ouverte pluridisciplinaire **HAL**, est destinée au dépôt et à la diffusion de documents scientifiques de niveau recherche, publiés ou non, émanant des établissements d'enseignement et de recherche français ou étrangers, des laboratoires publics ou privés.

# Water oxidation with inhomogeneous metal-silicon interfaces

Gabriel Loget

## Address

Univ Rennes, CNRS, ISCR (Institut des Sciences Chimiques de Rennes)-UMR6226, F-35000 Rennes, France. E-mail: [gabriel.loget@univ-rennes1.fr](mailto:gabriel.loget@univ-rennes1.fr)

## Abstract

Si is a prime candidate for manufacturing water-splitting photoelectrochemical cells, however, the stability of this material remains a serious bottleneck. This is particularly true for the photoanode, subject to severe deactivation mechanisms. So far, thin film homogeneity has been the paradigm in the quest for stable and efficient Si-based photoanodes, which involved the use of vapor deposition methods to produce conformal thin films ensuring Si protection and efficient catalysis during operation. Recent reports on *n*-Si/metal thin film junctions have highlighted the benefits of the junction heterogeneity, generated *in situ*. In addition, results obtained from *n*-Si photoanodes partially covered with discontinuous films of Co and Ni nanoparticles lately suggested that homogeneity is not a prerequisite to reach efficiency and stability. Such findings may open new protection routes for Si-based photoanodes, breaking with classical strategies and allowing the use of liquid phase modification methods such as electrodeposition.

## Abbreviations

ALD: atomic layer deposition

*cocat*: co-catalyst

MIS: metal-insulator-semiconductor

NP: nanoparticle

OER: oxygen evolution reaction

PEC: photoelectrochemical cell

SC: semiconductor

SCL: space charge layer

*Si/pc*: Si/co-catalytic protection layer

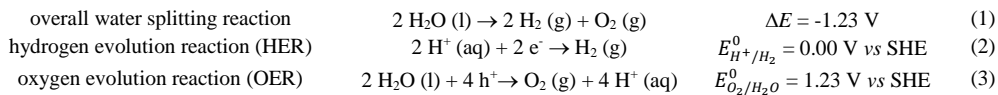
*Si/p/c*: Si/protection layer/co-catalyst

TCO: transparent conducting oxide

## 1 1-Introduction

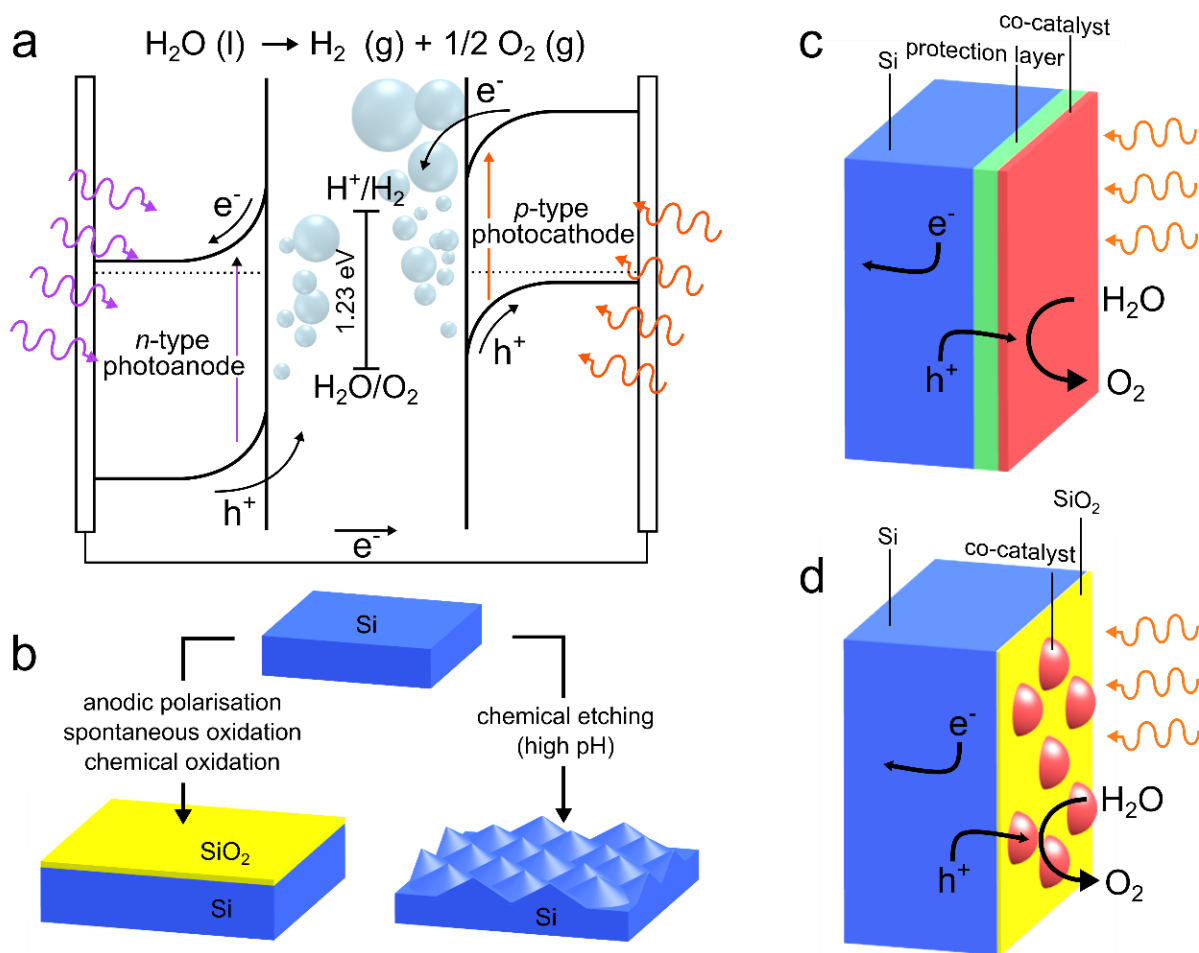
2 Although the integration of solar and wind energies in electrical grids is considerably growing  
3 worldwide, a major concern in employing these energy sources to a much larger extent is their  
4 intermittency and their diffuse geographic distribution. A solution to solve these two issues is the  
5 conversion of renewables into a carbon-free energy carrier that would allow the storage of energy and  
6 its distribution on site and on demand.[1] Hydrogen (H<sub>2</sub>) has long been considered as a highly  
7 promising energy carrier to fulfill this challenge in a carbon-neutral system, so-called the “hydrogen  
8 economy”.[2] In this view, solar and wind energies can be converted in H<sub>2</sub>, which would ensure in a  
9 perfect manner: energy storage as well as distribution and conversion in fuel cells, devices that readily  
10 convert H<sub>2</sub> into electricity with water being the only by-product.[3] To this goal, H<sub>2</sub> needs to be  
11 generated by the conversion of renewable energies through a zero-emission process. This is possible  
12 by coupling water electrolysis to a renewable source of energy to yield a completely clean and scalable  
13 process that generates highly pure H<sub>2</sub> only from water, as described by the overall reaction (1).[4]

14



15

16 In water electrolysis, the electrical current that is applied between two electrodes, immersed in water,  
17 breaks the chemical bonds of the water molecule, thus generating H<sub>2</sub> at the cathode (reaction (2)) and  
18 O<sub>2</sub> at the anode (reaction (3)). The latter reaction, referred to as oxygen evolution reaction (OER),  
19 requires the transfer of four charge carriers (photogenerated holes when an *n*-type photoanode is used)  
20 and four protons and is often considered the bottleneck of water electrolysis as it requires a  
21 considerable amount of energy to be triggered. In the specific case of solar energy conversion, the  
22 transformation of sunlight energy *via* the electrolysis of water can be achieved by two strategies. First,  
23 conversion and electrolysis can be performed by two independent and separated commercial devices,  
24 *i.e.*, a photovoltaic panel and an electrolyzer.[5,6] The second strategy combines both aspects on a  
25 single device, which can be done by interfacing sunlight-absorbing semiconductors (SCs) with an  
26 aqueous phase.[7–10] These systems are referred to as photoelectrochemical cells (PECs; Fig.1a) and  
27 have the advantage of being based on a simpler design that induces less potential losses and no power  
28 conditioning. Under sunlight irradiation the SC absorbs photons and convert them into charge carriers  
29 that are driven at the solid-liquid interface to react with water, generating pure H<sub>2</sub> (reaction (2)) and O<sub>2</sub>  
30 (reaction (3)). If the operation of relatively efficient PECs has been already demonstrated by different  
31 research groups,[11] several key challenges, such as their cost and their stability, need to be tackled to  
32 enable their practical use.[12]



1  
 2 **Fig.1.** a) Scheme showing a PEC made of a SC photoanode and a SC photocathode connected by an ohmic  
 3 contact. b) Scheme showing the deleterious mechanisms commonly occurring on Si photoelectrodes. c) Scheme  
 4 of a conventional Si photoanode in the Si/protection layer/co-catalyst (*Si/p/c*) configuration. d) Scheme of an  
 5 inhomogeneous MIS photoanode.

6 To be employed in PECs, SC absorbers must have: a short band gap to absorb a considerable part of  
 7 the sunlight and a high minority carrier lifetime. In this regard, silicon (Si) is particularly appealing  
 8 because it meets these standards. Moreover, it is very abundant (the 2<sup>nd</sup> element in the earth crust) and  
 9 widely used in the microelectronics and photovoltaic industries, which would be a great advantage for  
 10 technology transfer.[13] However, using Si as a photoelectrode, and particularly as a photoanode is  
 11 very challenging, because of *i*) its slow charge transfer kinetics for OER (reaction (3)) and *ii*) its  
 12 instability. The first problem is usually solved by integrating a high-efficiency co-catalyst (*cocat*) on  
 13 the Si surface which collects the photogenerated holes and improves OER kinetics. In this frame, a  
 14 particular interest is currently given to water electrolysis in alkaline medium because it allows  
 15 employing highly efficient OER *cocats*, based on cheap and abundant materials such as Fe, Mn, Co,  
 16 and Ni.[14] The latter issue (stability) has been the bottleneck for PEC manufacturing for long and is  
 17 still the subject of intense research.[15–17] As shown in Fig.1b, Si is subject to two main deleterious  
 18 mechanisms. The first one is the thermodynamic instability of Si, which passivates upon immersion in

1 aqueous solutions or when exposed to air with the spontaneous formation of an insulating native  
2 surface oxide. The anodic polarization of Si in aqueous medium intensifies this phenomenon which  
3 strictly prohibits the use of bare Si surface for OER.[18] The second degradation mechanism is Si  
4 etching, which happens readily at high pH, and prevents its use in alkaline solutions.[18] Over the last  
5 decades, tremendous progress has been made on developing modification strategies to fabricate  
6 efficient and stable Si-based photoanodes.[15,16] In this short review, we will first briefly present the  
7 classical protection strategies based on the use of conformal layers and we will then focus on an  
8 emerging type of Si-based photoanodes, referred to as inhomogeneous metal-insulator-semiconductor  
9 (MIS). We will present the recent research on that topic and discuss the advantages and drawbacks of  
10 such systems.

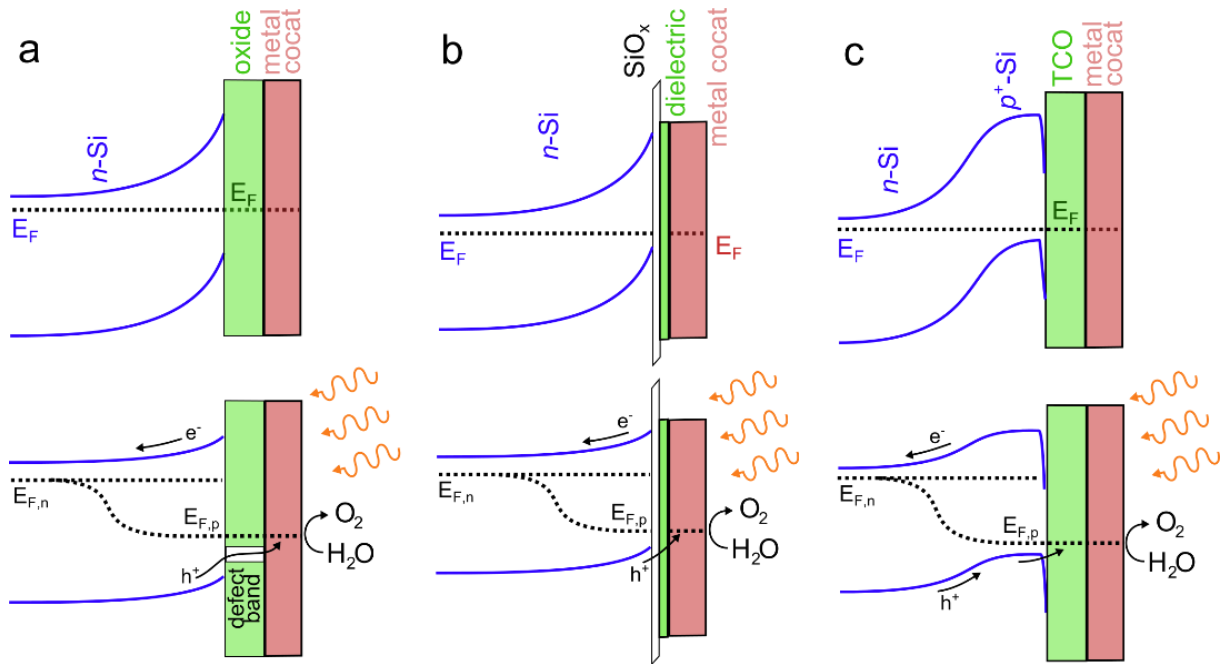
11

## 12 **2- Conformally coated Si photoanodes**

### 13 2-1- One layer for stability, the other one for activity

14 The protection of Si-based photoanodes implies, in most cases, the introduction of a conformal  
15 protection layer between the SC and the *cocat*, [15,16] deposited by means of chemical vapor  
16 deposition, physical vapor deposition or atomic layer deposition (ALD).[19] In order to design an  
17 efficient protection layer, drastic considerations must be taken into account. First, the coating should  
18 allow a charge flow by means of its intrinsic conductivity or by tunneling, it should not deteriorate the  
19 energetics of the interface and it should not impede light absorption. It is worth noting that several  
20 interesting examples of Si-based tandem photoanodes operating with a wide band gap SC acting as the  
21 same time as an absorber and as a Si protection coating have been reported but fall outside our  
22 scope.[20–23] In contrast, this short review focuses on the most commonly-employed Si protection  
23 strategies, implying oxide layers that absorb a minimal portion of the incident light but ensure  
24 protection and promote charge transfer from Si to the *cocat*. We herein refer to this construct as the  
25 Si/protection layer/co-catalyst (*Si/p/c*) configuration (Fig.1C). Note that in most of the cases, a thin  
26 (<2 nm) interfacial SiO<sub>x</sub> layer is also present at the Si surface. So far, TiO<sub>2</sub> has been the most  
27 employed material for Si protection. Several types of TiO<sub>2</sub>, prepared by different techniques and  
28 operating through different mechanisms, have been reported to be effective. Thick (up to 140 nm)  
29 layers of amorphous[24] and crystalline[25] TiO<sub>2</sub>, deposited by ALD on *n*-Si and interfaced with Ni-  
30 based *cocats* exhibit typical photovoltages of ~400 mV and could achieve OER with an unprecedented  
31 stability of 2,200 h.[26] In these systems, the solid Si/TiO<sub>2</sub> interface forms a buried junction[27] which  
32 controls the photovoltage and photogenerated holes are efficiently promoted through the “leaky” TiO<sub>2</sub>  
33 *via* electronic defects to the Ni which forms an ohmic contact with TiO<sub>2</sub> (Fig.2a).[24] Conversely,  
34 sputter-deposited crystalline Ti(5 nm)/TiO<sub>2</sub>(100 nm) protection layers were reported to only conduct  
35 electrons and to form ohmic contacts with *np*<sup>+</sup>-Si homojunction.[28] Furthermore, thin (~1-2 nm)

1 ALD-deposited  $\text{TiO}_2$  conformal coatings can behave as tunnel layers, allowing an efficient transfer of  
2 photogenerated charges when interfaced with an Ir *cocat* layer in a MIS configuration (Fig.2b).[29,30]  
3 Annealing these junctions with forming gas reduces the trap states density at the Si interface, which  
4 considerably increases the photovoltage.[31] In addition, a recent report revealed that integrating an  
5  $np^+$ -Si buried junction in such a MIS system allows to maintain a high interfacial hole density and to  
6 achieve an unprecedented photovoltage value of 630 mV.[32] Besides, thin ( $\sim 2$  nm) conformal  
7 dielectric films of ALD-deposited  $\text{HfO}_2$ [33] and  $\text{Al}_2\text{O}_3$ [31,34] have also been employed as dielectric  
8 layers in MIS photoanodes. In particular,  $\text{Al}_2\text{O}_3$ , in contact with an Ir *cocat* film, behaves as a tunnel  
9 oxide, implying an exponential increase of the device resistance as a function of its thickness.[31] In  
10 another recent study, the introduction of a high work function metal layer between the  $\text{Al}_2\text{O}_3$  tunnel  
11 layer and the Ni film allowed a considerable improvement of the barrier height, which resulted in  
12 photovoltages of  $\sim 530$  mV for optimized photoanodes.[35] In this case, the authors found that the  
13 maximum photovoltage was not obtained for the thinnest dielectric layer and did not exclude the  
14 possibility of defect-mediated carrier transport through the  $\text{Al}_2\text{O}_3$  film.[35] Finally, transparent  
15 conducting oxides (TCOs) have also been employed in the *Si/p/c* configuration. Only one example of a  
16 *p*-type TCO,  $\text{NiCo}_2\text{O}_4$ , has been reported in the *Si/p/c* configuration. This TCO was combined with an  
17  $np^+$ -Si buried junction and a NiFe-based OER *cocat* to perform OER for 72 h.[36] Mainly, classical *n*-  
18 type TCOs such as indium tin oxide (ITO)[37] or fluorine-doped  $\text{SnO}_2$  (FTO)[38] have been used for  
19 Si photoanode protection. In most of these reports, the TCOs have been employed with the aim of  
20 making non-rectifying electrical contact with a Si homojunction such as  $npp^+$ -Si,[37,38]  $np^+$ -Si [39] or  
21 with Si heterojunction cells,[40] in order to maintain the high photovoltage produced in the Si  
22 (Fig.2c). Thick (in the range of 100 nm) layers of sputtered ITO and FTO deposited by spray pyrolysis  
23 can protect the underlying Si when interfaced with OER *cocats*. These reports have however  
24 highlighted the disadvantages of this approach which are: *i*) the downward band bending at the ITO/Si  
25 interface that needs to be circumvented by employing a highly doped  $p^+$ -Si layer at the interface in  
26 order to ensure an efficient hole collection,[37] *ii*) the low hole conductivity of these *n*-type oxides[39]  
27 and *iii*) the low stability of ITO at harsh pH.[41] A recent very interesting report demonstrates that  
28 thick ( $\sim 100$  nm) layers of spray-deposited  $\text{SnO}_x$  on *n*-Si produces a high barrier heterojunction that can  
29 be employed for promoting OER with a photovoltage of  $\sim 620$  mV for 100 h when interfaced with  
30 highly-active OER *cocats*.[42]



1

2 **Fig.2.** Schematic band diagrams showing the charge transfer mechanisms occurring for the three main Si/p/c  
 3 configuration reported, after equilibration in the dark (top row) and in photoelectrochemical operation (bottom  
 4 row), the Fermi level ( $E_F$ ) of each component, as well as the hole ( $E_{F,p}$ ) and electron ( $E_{F,n}$ ) quasi-Fermi levels are  
 5 represented by dashed lines. a) The barrier height is imposed by the heterojunction formed between  $n$ -Si and the  
 6 thick oxide protecting layer, the *cocat* forms an ohmic contact with the oxide. The charge transfer from Si to the  
 7 *cocat* is achieved by charge conduction through the oxide layer (here, by hole conduction through defect bands).  
 8 b) The barrier height is imposed by the Schottky junction between  $n$ -Si and the metal *cocat*. This configuration is  
 9 referred to as MIS junction when the charge transfer from Si to the *cocat* occurs *via* tunneling through a thin  
 10 dielectric film. c) The barrier height is controlled by the buried  $np^+$ -Si homojunction. Efficient charge transfer at  
 11 the Si/TCO interface is usually promoted by employing a highly doped Si interfacial layer to reduce the thickness  
 12 of the interfacial space charge layer.

13 2-2- Combining protection and activity in a single layer

14 An alternative and highly beneficial strategy that has also been employed to decrease the  
 15 manufacturing costs consists in employing a coating material that acts as a Si protection layer and, as  
 16 the same time, as a *cocat*. We refer here to this configuration as Si/co-catalytic protection layer (*Si/pc*).  
 17 Note that in such a configuration, even though only one layer is deposited over the Si surface, an  
 18 additional conditioning step of the surface is often required to generate catalytic species on that layer,  
 19 sometimes that step is spontaneously occurring during OER. Therefore, if the *Si/pc* is more attractive  
 20 than the *Si/p/c* configuration in terms of fabrication, these systems are, *in fine*, relatively identical from  
 21 a structural point of view. Interestingly, only one recent report has described a *Si/pc* photoanode  
 22 operating at low pH (employing an Ir-based film on  $np^+$ -Si).[43] In contrast, the use of the *Si/pc*  
 23 configuration for photoanodes operating at high pH has been lately investigated by several groups. If  
 24 this may first seem unexpected considering the fact that alkaline media are harsher for Si (Fig.1b) it  
 25 can be explained by the fact that these conditions allow employing abundant OER-active materials  
 26 (based on Fe, Mn, Co, and Ni).[14] So far, very little has been reported on  $FeO_x$ [44] and  $MnO_x$ [45]  
 27 layers, which, when employed as films in the range of  $\sim 10$  nm on  $n$ -Si, are known to promote OER

1 with photovoltages partially controlled by the liquid phase. [44,45] More work has been focused on  
2  $\text{CoO}_x$  layers, for instance, thin (~2-5 nm)  $\text{CoO}_x$  layers deposited by plasma-enhanced ALD or  
3 sputtering have been employed to protect crystalline[46] or amorphous Si homojunctions.[47] In  
4 particular, annealing these films allowed to generate a catalytically-active  $\text{Co}(\text{OH})_2$  outer layer on the  
5 top of a dense and highly impermeable  $\text{Co}_3\text{O}_4$  which was very efficient on  $np^+$ -Si.[48] Thicker (~50  
6 nm), ALD-deposited  $\text{CoO}_x$  coatings have been also employed on  $n$ -Si with which they form a  
7 heterojunction affording a ~570 mV photovoltage and can protect the system for 100 days of  
8 continuous electrolysis.[49] Most of the *Si/pc* systems are based on Ni layers. If it has been reported  
9 that ~75 nm-thick transparent and antireflective  $\text{NiO}_x$  layers (deposited by reactive sputtering)  
10 generate a rather low barrier heterojunction with  $n$ -Si (and can only afford a ~200 mV photovoltage  
11 for OER),[50] it can be considerably improved by incorporating a  $\text{CoO}_x$  interlayer.[51] Such  $\text{NiO}_x$   
12 coatings can be employed as conductive, protective and catalytic layers for crystalline[50] and  
13 amorphous[52] Si homojunctions as well as Si heterojunctions.[52] In addition, sputtered, ~50 nm-  
14 thick  $\text{NiO}$ [53] and  $\text{NiCoO}_x$ [54] have been used as  $p$ -type conductive catalytic layers to protect  $np^+$ -  
15 and back-illuminated  $n^+pp^+$ -Si homojunctions. It has been clearly shown that the electrochemical  
16 performance of these layers is affected by the presence of Fe in solution and have been employed for  
17 300[53] and 72 h[54] of operation, respectively. It is worth noting that the deliberate or unintentional  
18 doping of Ni-based coatings with Fe atoms (that can originate from the materials employed during  
19 water electrolysis experiments) is quite important as Fe is known to strongly affect the catalytic  
20 performance of Ni-based catalysts, for instance, it integrates into the highly-active OER phase  $\text{NiOOH}$   
21 to produce  $\text{Ni}(\text{Fe})\text{OOH}$ , that can lead to an improvement or a degradation of the OER thermodynamics  
22 and kinetics, depending on the Fe content.[77] Thin Ni metal layers, deposited by e-beam or thermal  
23 evaporation on  $n$ -Si, have also been employed for manufacturing *Si/pc* photoanodes. The first  
24 publication on this system reported the considerable effect of the layer thickness on the  
25 photoelectrochemical properties as well as the importance of the interfacial  $\text{SiO}_x$  layer.[55] Optimal  
26 performance was obtained for 2 nm-thick films which afforded ~500 mV photovoltage and 12 h  
27 stability at pH 14. This photovoltage value is much higher than the one expected for a classical  $n$ -  
28 Si/ $\text{SiO}_x$ /Ni Schottky barrier and this striking behavior, obtained for such a simple system, has triggered  
29 a broad interest. In particular, it has been recently shown that the failure is caused by the thickening of  
30 the  $\text{SiO}_x$ ,[56] associated with the permeation of the Ni/ $\text{NiO}_x$  during operation. The  $n$ -Si/ $\text{SiO}_x$ /Ni  
31 photoanodes have been first described as a classical MIS device (Fig.2b) where the partially oxidized  
32 Ni layer homogeneously coat Si, but, with a particular case for ultrathin layers (2 nm) where  $n$ -Si  
33 equilibrates with both the Ni and the liquid phase, affording the higher built-in potential.[55] If this  
34 description has been confirmed for thick Ni layer,[57,58] a recent study employing the dual working  
35 electrode technique (which allows decoupling the electrochemical activity of the coating from the  
36 overall photoanode response) allowed to get more insights on the operating mechanism of  $n$ -Si  
37 photoanodes coated with ultrathin Ni layers.[58] First, it revealed that the junction controlling the

1 photovoltage is buried and dynamic as it is not influenced by the solution potential but evolves during  
2 electrochemical conditioning. However, it clearly pointed out that the activity of this system was not  
3 entirely controlled by the chemical transformation of Ni to a more active *cocat* phase during  
4 conditioning, but is mostly due to a structural change at the solid/solid interface.[58] It was proposed  
5 that during activation the majority of the Ni<sup>0</sup> layer was converted into Ni(OH)<sub>2</sub> which is OER active,  
6 but, more importantly, permeable to the electrolyte, causing the anodization of Si to insulating SiO<sub>x</sub> in  
7 the regions of contact with the electrolyte. Besides, X-ray photoelectron spectroscopy revealed the  
8 presence of Ni<sup>0</sup> remaining in the film. These elements allowed a better understanding of this surface,  
9 considered now as an inhomogeneous buried junction operating in the pinch-off regime, as shown in  
10 Fig.3c (note that pinch-off will be described in section 3-2).

11

### 12 **3- Inhomogeneously coated Si photoanodes**

#### 13 3-1- Inhomogeneous photoanodes not in the pinch-off regime

##### 14 3-1-1- Photoanodes patterned by vapor deposition

15 Using arrays of micrometer-sized *cocat* patterns in contact with Si instead of conformal films can be  
16 advantageous for reducing optical losses and improving light absorption by the SC. Furthermore, the  
17 protection of the uncoated surface can be addressed quite conveniently by oxidizing the uncovered Si  
18 to generate a passive SiO<sub>x</sub> layer. Several interesting examples of inhomogeneous Si photoanodes  
19 patterned with arrays of micrometer-sized *cocat* patches (larger than the SCL, thus not exhibiting  
20 pinch-off, see section 3-2), fabricated by a combination of clean room and physical vapor deposition  
21 techniques have been reported. For instance, Ni deposited directly on *n*- or *np*<sup>+</sup>-Si(111), can be  
22 employed as micro-sized catalytic patches to promote OER for durations exceeding 100 h at pH  
23 14.[59] In this case, the anodic SiO<sub>x</sub> generated *in situ* protects the uncoated Si during operation. This  
24 design has been employed for monitoring the local O<sub>2</sub> production and identifying the photoanode  
25 failure modes. Another strategy consists in patterning a Si surface that is initially passivated with a  
26 thick SiO<sub>2</sub> thermal oxide layer to ensure a long-term stability. This concept has been employed with  
27 arrays of Pt and Ti/Ni planar disks[60] as well as nanostructured Au/Ni and Au/NiFe micro-sized  
28 islands[61] on *np*<sup>+</sup>-Si for OER at alkaline pH. In these cases, however, the use of reactive ion etching  
29 is required to regioselectively remove the SiO<sub>2</sub> before metal deposition. An attractive and original  
30 method based on localized dielectric breakdown can be employed to circumvent this technical issue. It  
31 has been shown that micrometer-sized islands of a NiFe-based *cocat*, deposited by e-beam evaporation  
32 directly on a 30 nm-thick thermally grown SiO<sub>2</sub>, can be electrically contacted to the underlying *n*-Si by  
33 exceeding the breakdown voltage. Such a procedure allows creating a conducting filament between the  
34 *cocat* island and the SC that promotes the conduction of photogenerated holes through the  
35 dielectric.[62]

### 1            3-1-2- Photoanodes prepared by electrochemical methods

2    Almost all photoanode designs discussed in the previous sections require high vacuum deposition  
3    techniques. Alternative solution-based methods would not be only attractive from a financial point of  
4    view but also because they may offer new possibilities in terms of coating composition or  
5    morphology. Pioneer research has been carried out in that direction using sol-gel processes to protect  
6    *n*-Si but resulted in limited stability.[63] Modification techniques based on electrochemistry, such as  
7    electrodeposition, seems particularly attractive because they are usually low-cost, can be employed to  
8    deposit a wide variety of materials on conductors or SCs and they usually allow a precise control over  
9    the film thickness. Even though electrochemical techniques such as electrodeposition and anodization  
10   were early suggested to prepare Si-based photoanodes,[64] they have been scarcely employed so far,  
11   probably due to the well-established instability of Si surfaces in liquid electrolytes and the fear of  
12   generating a fully-insulating SiO<sub>x</sub> layer during surface modification (section 1). In addition, high  
13   vacuum techniques are usually preferred as they typically produce high density and pinhole-free  
14   coatings, which is not always the case for electrodeposited layers, at the expense of long-term stability.  
15   However, in view of the recent knowledge on the Si/electrolyte interface and the interest given on the  
16   pinch-off effect (see section 3-2), it does not seem worthless to explore the use of electrochemical  
17   processes applied to the manufacturing of Si-based photoanodes, and experimental works readily  
18   revealed that such methods could lead to photoanodes with remarkable performance. In the following,  
19   we will first describe the very few examples using electrochemical methods (mostly electrodeposition)  
20   to fabricate Si-based photoanodes that are not operating in the pinch-off regime and we then will  
21   discuss the fabrication of pinched-off photoanodes (next section). Recently, electrodeposition of  
22   inhomogeneous metal layers has been employed to produce photoanodes in the *Si/pc* configuration to  
23   protect Si buried homojunctions. Thin (~6 nm) and discontinuous NiFe metal films exhibited great  
24   performance on *np*<sup>+</sup>-Si, which afforded a photovoltage of 620 mV and a stability >12 h at pH 14.[65]  
25   In addition, the scalability of electrochemical processes applied to Si-based materials has been  
26   demonstrated by a recent publication that reported the electrodeposition of large and flexible NiFe  
27   films and their subsequent anodization via a continuous roll-to-roll process to form a highly active  
28   OER *cocat* layer. Its integration to an amorphous Si solar cell has allowed oxidizing water in 1 M  
29   KOH from on onset potential as low as +0.6 V vs RHE and an operation time of 12 h.[66]

### 30    3-2- Pinched-off photoelectrodes

31   The pinch-off phenomenon has been first introduced in the field of solid state physics as a way to  
32   explain the behavior of inhomogeneous Schottky junctions.[67] In such a typical system, the SC  
33   surface is brought in contact with two phases leading to an inhomogeneity of the depletion region. If  
34   these systems were previously typically considered as separated heterojunctions operating in parallel,  
35   several results revealed the non-validity of this model when the characteristic size of one junction  
36   became comparable or fell below the thickness of the space-charge layer (SCL).[68] This size effect

1 has been attributed to the pinch-off effect in the early eighties,[69] and was rationalized in the  
2 nineties.[70] The pinch-off effect is illustrated by Fig.3b in the case of a low-doped *n*-Si surface that  
3 contains two interfaces of different barrier heights: a low barrier region, spatially distributed in areas  
4 of a characteristic size smaller than the SCL and a high barrier region that covers the rest of the Si  
5 surface. In this size regime, the depletion of majority carriers required to reach equilibrium at the high  
6 barrier contact extends under the low barrier contact, affecting the local band bending (creating a  
7 “saddle point” under the high barrier-region) and increases the overall barrier height (Fig.3a vs  
8 Fig.3b).[67] The pinch-off effect has been early observed in the case of inhomogeneous *n*-Si/metal  
9 junction in contact with liquid phases.[71,72] Notably, a study has shown that the behavior of *n*-Si  
10 covered with Ni patches immersed in an organic electrolyte containing a reversible redox couple (to  
11 create a high barrier Si/electrolyte region at the Ni-free regions) behaves in good agreement with the  
12 pinch-off theoretical predictions when the Ni patch size was below 100 nm.[73] It is obvious that the  
13 pinch-off effect can be very advantageous to fabricate Si-based OER photoanodes and compensate the  
14 losses caused by Fermi-level pinning, often generated at SC/metal junctions. In addition, it combines  
15 very well with the hydrogenated Si (Si-H) surface for which surface energetics can be finely tuned by  
16 chemical surface functionalization.[74] More importantly, interfacial SiO<sub>x</sub> can be easily employed to  
17 passivate Si and generate a high barrier region with a low density of interface states. Thus, pinched-off  
18 photoelectrodes could be, in principle, easily fabricated by partially modifying Si with small particles  
19 of an appropriate metal and oxidizing the non-coated area. In addition to the high photovoltage  
20 generated by the effect, in this configuration, the photogenerated holes will mainly flow through the  
21 less resistive pathway and will be collected at the metal particles where they can be employed for  
22 OER.

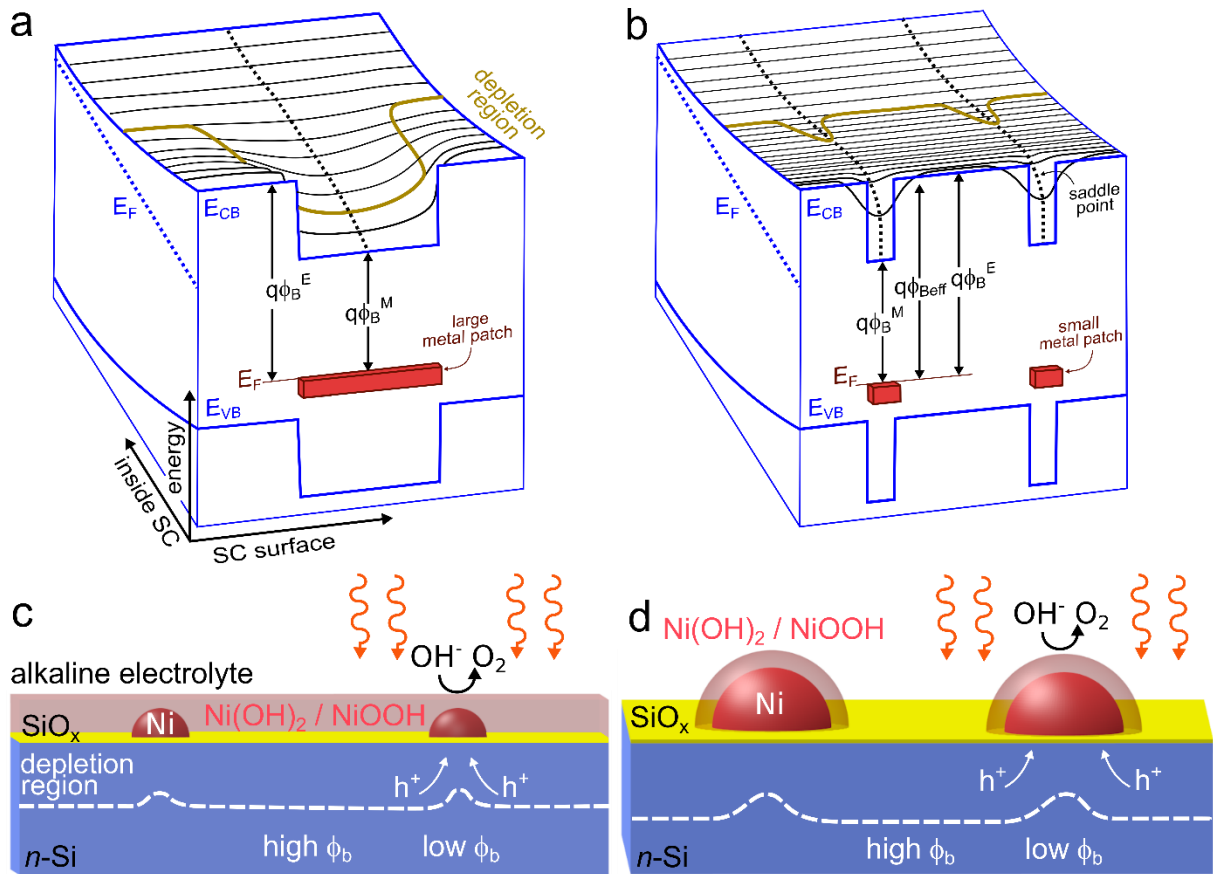


**Fig.3.** a,b) Schematic energy diagrams, adapted from Nakato *et al.* (reference[72]), for a *n*-type SC in contact with a metal patch that produces a low barrier height ( $\phi_B^M$ ) region and a second phase that produces a high barrier height ( $\phi_B^E$ ) region ( $q$  is the elementary charge). In a) the metal patch is large and in b) the metal patch is small with respect to the depletion width. In blue are represented the energies of the Fermi level ( $E_F$  dotted line), the valence band ( $E_{VB}$ ) and the conduction band ( $E_{CB}$ ) of the SC and in red is represented the  $E_F$  of the metal. The full black lines represent the distribution of the potential barrier inside the SC, the dotted black line represent the potential distribution under a metal patch and the dark yellow line represent the depletion region. In Fig.3b, because of the small size of the metal patches, the surface is pinched-off and the effective barrier height ( $\phi_{B\text{eff}}$ ) is much higher than  $\phi_B^M$ . c) Scheme, adapted from Boettcher *et al.* (reference [58]), showing the interface of an *n*-Si/SiO<sub>x</sub>/Ni, where the Ni is ultrathin. During operation, the Ni surface is partially converted in catalytic and permeable Ni(OH)<sub>2</sub>/NiOOH, allowing Si to oxidize and to form a SiO<sub>x</sub> passive layer. This surface is thought to be pinched-off (as in Fig.3b), explaining the high value of obtained photovoltages. d) Scheme showing the interface of a pinched-off inhomogeneous MIS photoanode fabricated by electrodeposition of Ni<sup>0</sup> on *n*-Si (section 3-3).

### 3-3- Pinched-off photoanodes prepared by electrochemical methods

Typical cathodic electrodeposition of metals occurs *via* a nucleation-growth mechanism which makes this method particularly relevant for the decoration of an *n*-Si surface with dispersed metal nanoparticles (NPs), causing a minimal light interference and inducing the pinch-off phenomenon. The first example of a rather stable (~2 h at pH 14 and 25 h at pH 9) photoanode composed of nanometer-sized metal electrodeposits on *n*-Si was reported in 2015. Here, inhomogeneous Co islands were reported to generate high photocurrents (> 30 mA cm<sup>-2</sup>) and surprisingly high photovoltages, greater than the one obtained with conformal *n*-Si/CoSi<sub>2</sub> and *n*-Si/SiO<sub>x</sub>/Co solid junctions.[75] If the authors

1 could not ascribe this behavior to a precise physical phenomenon, they clearly demonstrated the  
2 importance of *i*) the Co inhomogeneity to generate different barrier heights and *ii*) the SiO<sub>x</sub> layer, and,  
3 showed that the photovoltage was independent of the solution potential. In addition, they also  
4 suggested that the CoOOH catalytic layer, formed around the Co<sup>0</sup> particles could play a role in the  
5 interface energetics and may improve charge extraction.[75] This report set an important landmark as  
6 it showed for the first time that electrodeposited inhomogeneous coatings can be used to fabricate  
7 photoanodes with remarkable performance without employing a buried Si homojunction and a  
8 homogeneous protection layer. Two years later, we have demonstrated that *n*-Si modified with  
9 dispersed hemispherical Ni NPs by cathodic electrodeposition can be employed to trigger OER in  
10 alkaline media with an onset potential more negative than the O<sub>2</sub>/H<sub>2</sub>O formal potential and a higher  
11 stability[76] than those previously reported for Co-based electrodes.[75] We have also evidenced a  
12 strong correlation between the Ni coverage and the photoelectrochemical performance. Indeed, the  
13 highest photovoltages and photocurrents were obtained for low Ni coverage while an increase of the  
14 Ni loading decreased the performances (but increased the stability). The electrodes fabricated using  
15 this method exhibit photovoltages that can exceed 400 mV and can operate for more than 10 h at pH  
16 14.[76] Actually, the behavior of these photoanodes is very similar to that reported for ultrathin  
17 conformal layers of Ni (described in section 2-2, see Fig.3c), which suggests that both of them are  
18 operating in the pinch-off regime, as shown in Fig.3d.[55] We recently reported the effect of  
19 photoelectrochemical activation, which, by producing a catalytic Ni(OH)<sub>2</sub>/NiOOH shell, doped with  
20 Fe (thus referred here as Ni(Fe)(OH)<sub>2</sub>/Ni(Fe)OOH), around the Ni<sup>0</sup> particles, can considerably  
21 improve the OER kinetics.[77] In addition, a stability study revealed that the protection originates  
22 from the oxidation of the uncoated Si which readily passivates the Si exposed to the solution and  
23 protects it, *in operando*, from alkaline etching. Besides, unexpected stability was reported at the open  
24 circuit potential and it was found that the presence of the Ni particles on the surface slowed down  
25 electrode deactivation with a more pronounced effect under illumination.[77] After our initial report,  
26 several groups have employed the same strategy to fabricate pinched-off photoanodes. For instance,  
27 the effect of annealing was studied and the thermal oxidation of the Ni particles was found to improve  
28 the photovoltage and the photocurrent, which was attributed to the partial conversion of Ni to a *p*-type  
29 NiO<sub>x</sub> that increased the pinched-off barrier height underneath the Ni NPs.[78] An interesting study has  
30 reported the effect of the thickness of the Ni(OH)<sub>2</sub> layer grown on the Si NPs. In this case, the  
31 Ni(OH)<sub>2</sub> was electrochemically deposited over the Ni particles,[79] which produced essentially the  
32 same effect as electrochemical conditioning,[77] except that the Ni core remained unaffected during  
33 deposition. It was shown that the presence of the Ni(OH)<sub>2</sub> coating considerably improved the open  
34 circuit photovoltage and therefore the performance for OER. Ni(OH)<sub>2</sub> was assumed to be responsible  
35 for the increase in the overall barrier height due to a *p*-type nature,[79] which may be the subject of  
36 debate because Ni(OH)<sub>2</sub> is typically insulating and electrolyte permeable.[80] Also, this  
37 electrodeposition process has been applied to microstructured *n*-Si.[81] Recently, we have reported the

1 integration of these pinched-off photoanodes in an “all Si”-based monolithic photoelectrochemical cell  
2 that quantitatively produced H<sub>2</sub> directly under solar illumination,[82] showing that this type of  
3 photoanode can be employed for unassisted solar water splitting.

4 Furthermore, owing to the very negative redox potential of the SiO<sub>2</sub>/Si couple, bare Si can be directly  
5 employed to reduce certain metal salts at its surface without applying an external bias. Although being  
6 of an electrochemical nature, this process, referred to as electroless deposition, is spontaneous and  
7 does not require the use of a potentiostat. It has been recently employed to spontaneously modify *n*-Si  
8 with Ni particles,[83] leading to photoanodes with a considerably different structure as, in this case, a  
9 submicrometer-thick porous SiO<sub>2</sub> layer comprising conductive Ni filaments was formed between the  
10 Si and the Ni *cocatalyst* during the electroless deposition process. Interestingly, the reported  
11 photoelectrochemical properties of these photoanodes were very similar to those obtained by Ni  
12 cathodic electrodeposition, suggesting that the pinch-off effect might also happen at the  
13 Si/inhomogeneous Ni-SiO<sub>2</sub> interface despite structural differences and the interface complexity.

14

#### 15 **4- Concluding remarks**

16 Si-based water-splitting PECs could potentially play a role in a sustainable energy economy, however,  
17 this would be only feasible if the current bottlenecks that are: *i*) their cost and *ii*) their stability are  
18 successfully addressed. In order to overcome this challenge, considerable research effort has been  
19 made on Si-based photoanodes, that suffer from serious deleterious mechanisms, leading to their fast  
20 deactivation (section 1). So far, homogeneity has been the paradigm in the search for stable and  
21 efficient Si-based photoanodes, which involved the use of physical vapor deposition, chemical vapor  
22 deposition or ALD to produce conformal, pinhole-free, oxide thin films ensuring Si protection and  
23 efficient catalysis during operation (section 2). The recent progress in this area has been considerable,  
24 as demonstrated by several reports showing the operation of highly stable Si-based photoanodes with  
25 operation time in the range of 100 h and up to more than 2,000 h.[26]

26 On the other hand, recent reports on photoanodes based on the MIS configuration have shown that,  
27 when properly engineered,[32,35] such interfaces can exhibit excellent OER performance,  
28 approaching the one obtained with buried Si homojunctions. The interest of these studies is twofold as  
29 they may potentially decrease the process costs related to the fabrication of Si-based photoanodes by  
30 avoiding the need for homojunctions and also because they point out principles that may be transposed  
31 to other SC materials, for which homojunctions cannot be created. A remarkable example in the frame  
32 of Si/metal junction is the *n*-Si/Ni junction,[55] which is prepared by coating *n*-Si with an ultrathin  
33 layer of Ni. Although this junction is initially homogeneous, a recent experimental study has shown  
34 that its outstanding performance originates from its inhomogeneity, which is generated during  
35 operation.[58] It is, thus, intriguing to note that considerable improvement can arise from the

1 transformation of a homogeneous phase to a highly inhomogeneous (and partially electrolyte-  
2 permeable) phase while keeping a decent stability. Such findings should trigger the interest in novel  
3 forms of protection, breaking with the classical strategies, which could involve simpler liquid-phase  
4 fabrication methods.

5 In this context, electrochemical modification methods may be perfect candidates for preparing  
6 efficient water-splitting photoanodes. This has been recently suggested by recent reports on randomly-  
7 dispersed Co[75] and Ni[76,77] NP arrays, generated by electrodeposition on *n*-Si. In these systems, a  
8 large portion of the Si is exposed to the electrolyte, which induces its anodic passivation under  
9 operation and favors pinch-off (section 3-2), promoting high built-in voltages. The simplicity of Ni  
10 electrodeposition has quickly driven several research groups to employ this method successfully which  
11 has led to stability in the range of 10 h at pH ~14[76] and up to 300 h at pH 9.[79] Such a stability  
12 could first seem unexpected considering such corrosive environments for Si, and that the largest Si  
13 part is covered by nothing but its anodic oxide. If these unexpected recent reports are exciting, the  
14 performance of inhomogeneous photoanodes manufactured this way is still far from their conformal,  
15 oxide-coated, counterparts in terms of photovoltage[42] but also stability.[26] Nevertheless, it is  
16 expected that considerable progress could be obtained through a better understanding of the pinch-off  
17 effect as well as a fine characterization of the Si/metal, Si/SiO<sub>x</sub> and SiO<sub>x</sub>/metal interfaces, that all seem  
18 to play an important role for photovoltage generation and stability.[77] A detailed comprehension of  
19 each component of these complex inhomogeneous surfaces may open doors for improvement of the  
20 photoanode lifetime. It is envisioned that ameliorations are within reach by applying simple chemical  
21 treatments, for instance, improving the oxide quality or generating interfacial silicides.  
22 Electrodeposition conveniently allows triggering layer by layer modifications at the *cocat* level  
23 (allowing the generation of core-shell structures) and thus, is expected to quickly lead to progress in  
24 the optimization the catalytic aspect of these photoanodes.[77,79,84] In addition, progress will  
25 probably arise from studying other important considerations such as *cocat* geometry, adhesion, and  
26 surface distribution. Attention should also be paid to a crucial but often neglected aspect that is the  
27 photoanode stability when unbiased. Indeed, all photoanodes described in this short review are  
28 expected to be integrated into water-spitting PECs where they will be subject to dark cycles (typically  
29 overnight) which may be strongly deleterious to, especially at high pH.

### 30 **Funding**

31 This work is partly funded by ANR (project EASi-NANO, ANR-16-CE09-0001-01)

### 32 **Acknowledgments**

33 Dr. Bruno Fabre is warmly acknowledged for fruitful discussions.

### 34 **References**

35 **Papers of special interest (•):** refs [13],[16],[24],[32],[35],[58],[70],[73],[76],[79],[82]

- 1 **Papers of outstanding interest (••):** refs [55],[75]
- 2 1. Elliott D: **A balancing act for renewables.** *Nat Energy* 2016, **1**:15003.
- 3 2. Bockris JO: **A hydrogen economy.** *Science* 1972, **176**:1323–1323.
- 4 3. Stamenkovic VR, Strmcnik D, Lopes PP, Markovic NM: **Energy and fuels from electrochemical**  
5 **interfaces.** *Nat Mater* 2017, **16**:57–69.
- 6 4. Xiang C, Papadantonakis M, Lewis NS: **Principles and implementations of electrolysis systems**  
7 **for water splitting.** *Mater Horizons* 2016, **3**:169–173.
- 8 5. Cox CR, Lee JZ, Nocera DG, Buonassisi T: **Ten-percent solar-to-fuel conversion with**  
9 **nonprecious materials.** *Proc Natl Acad Sci USA* 2014, **111**:14057–14061.
- 10 6. Luo J, Im J-H, Mayer MT, Schreier M, Nazeeruddin MK, Park N-G, Tilley SD, Fan HJ, Grätzel M:  
11 **Water photolysis at 12.3% efficiency via perovskite photovoltaics and earth-abundant**  
12 **catalysts.** *Science* 2014, **345**:1593–1596.
- 13 7. Fujishima A, Honda K: **Electrochemical photolysis of water at a semiconductor electrode.**  
14 *Nature* 1972, **238**:37–38.
- 15 8. Gerischer H: **Solar photoelectrolysis with semiconductor electrodes.** In *Solar Energy*  
16 *Conversion: Solid-State Physics Aspects.* Edited by Seraphin BO. Springer; 1979:115–172.
- 17 9. Walter MG, Warren EL, McKone JR, Boettcher SW, Mi Q, Santori EA, Lewis NS: **Solar water**  
18 **splitting cells.** *Chem Rev* 2010, **110**:6446–6473.
- 19 10. Sivula K, van de Krol R: **Semiconducting materials for photoelectrochemical energy**  
20 **conversion.** *Nat Rev Mater* 2016, **1**:15010.
- 21 11. Ager JW, Shaner MR, Walczak KA, Sharp ID, Ardo S: **Experimental demonstrations of**  
22 **spontaneous, solar-driven photoelectrochemical water splitting.** *Energy Environ Sci* 2015,  
23 **8**:2811–2824.
- 24 12. Shaner MR, Atwater HA, Lewis S, McFarland EW: **A comparative technoeconomic analysis of**  
25 **energy.** *Energy Environ Sci* 2016, **9**:2354–2371.
- 26 13. Sun K, Shen S, Liang Y, Burrows PE, Mao SS, Wang D: **Enabling silicon for solar-fuel**  
27 **production.** *Chem Rev* 2014, **114**:8662–8719.
- 28 14. McCrory CCL, Jung S, Ferrer IM, Chatman SM, Peters JC, Jaramillo TF: **Benchmarking hydrogen**  
29 **evolving reaction and oxygen evolving reaction electrocatalysts for solar water splitting**  
30 **devices.** *J Am Chem Soc* 2015, **137**:4347–4357.
- 31 15. Hu S, Lewis NS, Ager JW, Yang J, McKone JR, Strandwitz NC: **Thin-film materials for the**  
32 **protection of semiconducting photoelectrodes in solar-fuel generators.** *J Phys Chem C* 2015,  
33 **119**:24201–24228.
- 34 16. Bae D, Seger B, Vesborg PCK, Hansen O, Chorkendorff I: **Strategies for stable water splitting**  
35 **via protected photoelectrodes.** *Chem Soc Rev* 2017, **46**:1933–1954.
- 36 17. Chen S, Wang L-W: **Thermodynamic oxidation and reduction potentials of photocatalytic**  
37 **semiconductors in aqueous solution.** *Chem Mater* 2012, **24**:3659–3666.
- 38 18. Zhang XG: *Electrochemistry of Silicon and Its Oxide.* Kluwer Academic; 2001.
- 39 19. Yu Y, Zhang Z, Yin X, Kvit A, Liao Q, Kang Z, Yan X, Zhang Y, Wang X: **Enhanced**  
40 **photoelectrochemical efficiency and stability using a conformal TiO<sub>2</sub> film on a black silicon**

- 1 **photoanode**. *Nat Energy* 2017, **2**:17045.
- 2 20. Ao X, Tong X, Kim DS, Zhang L, Knez M, He S, Schmidt V: **Black silicon with controllable**  
3 **macropore array for enhanced photoelectrochemical performance**. *Appl Phys Lett* 2012,  
4 **101**:111901.
- 5 21. Shaner MR, Fountaine KT, Ardo S, Coridan RH, Atwater HA, Lewis NS: **Photoelectrochemistry**  
6 **of core-shell tandem junction n-p<sup>+</sup>-Si/n-WO<sub>3</sub> microwire array photoelectrodes**. *Energy*  
7 *Environ Sci* 2014, **7**:779–790.
- 8 22. Santinacci L, Diouf MW, Barr MKS, Fabre B, Joanny L, Gouttefangeas F, Loget G: **Protected**  
9 **light-trapping silicon by a simple structuring process for sunlight-assisted water splitting**.  
10 *ACS Appl Mater Interfaces* 2016, **8**:24810–24818.
- 11 23. Chakthranont P, Hellstern TR, McEnaney JM, Jaramillo TF: **Design and fabrication of a**  
12 **precious metal-free tandem core-shell p<sup>+</sup>n Si/W-doped BiVO<sub>4</sub> photoanode for unassisted**  
13 **water splitting**. *Adv Energy Mater* 2017, **7**:1701515.
- 14 24. Hu S, Shaner MR, Beardslee JA, Lichterman M, Brunenschwig BS, Lewis NS: **Amorphous TiO<sub>2</sub>**  
15 **coatings stabilize Si, GaAs, and GaP photoanodes for efficient water oxidation**. *Science* 2014,  
16 **344**:1005–1009.
- 17 25. McDowell MT, Lichterman MF, Carim AI, Liu R, Hu S, Brunenschwig BS, Lewis NS: **The influence**  
18 **of structure and processing on the behavior of TiO<sub>2</sub> protective layers for stabilization of n-**  
19 **Si/TiO<sub>2</sub>/Ni photoanodes for water oxidation**. *ACS Appl Mater Interfaces* 2015, **7**:15189–  
20 15199.
- 21 26. Shaner MR, Hu S, Sun K, Lewis NS: **Stabilization of Si microwire arrays for solar-driven H<sub>2</sub>O**  
22 **oxidation to O<sub>2</sub>(g) in 1.0 M KOH(aq) using conformal coatings of amorphous TiO<sub>2</sub>**. *Energy*  
23 *Environ Sci* 2015, **8**:203–207.
- 24 27. Hu S, Richter MH, Lichterman MF, Beardslee J, Mayer T, Brunenschwig BS, Lewis NS: **Electrical,**  
25 **photoelectrochemical, and photoelectron spectroscopic investigation of the interfacial**  
26 **transport and energetics of amorphous TiO<sub>2</sub>/Si heterojunctions**. *J Phys Chem C* 2016,  
27 **120**:3117–3129.
- 28 28. Mei B, Pedersen T, Malacrida P, Bae D, Frydendal R, Hansen O, Vesborg PCK, Seger B,  
29 Chorkendorff I: **Crystalline TiO<sub>2</sub>: a generic and effective electron-conducting protection layer**  
30 **for photoanodes and -cathodes**. *J Phys Chem C* 2015, **119**:15019–15027.
- 31 29. Chen YW, Prange JD, Dühnen S, Park Y, Gunji M, Chidsey CED, McIntyre PC: **Atomic layer-**  
32 **deposited tunnel oxide stabilizes silicon photoanodes for water oxidation**. *Nat Mater* 2011,  
33 **10**:539–544.
- 34 30. Scheuermann AG, Prange JD, Gunji M, Chidsey CED, McIntyre PC: **Effects of catalyst material**  
35 **and atomic layer deposited TiO<sub>2</sub> oxide thickness on the water oxidation performance of**  
36 **metal-insulator-silicon anodes**. *Energy Environ Sci* 2013, **6**:2487–2496.
- 37 31. Scheuermann AG, Kemp KW, Tang K, Lu DQ, Satterthwaite PF, Ito T, Chidsey CED, McIntyre  
38 PC: **Conductance and capacitance of bilayer protective oxides for silicon water splitting**  
39 **anodes**. *Energy Environ Sci* 2016, **9**:504–516.
- 40 32. Scheuermann AG, Lawrence JP, Kemp KW, Ito T, Walsh A, Chidsey CED, Hurley PK, McIntyre  
41 PC: **Design principles for maximizing photovoltage in metal-oxide-protected water-splitting**  
42 **photoanodes**. *Nat Mater* 2016, **15**:99–105.
- 43 33. Quinn J, Hemmerling J, Linic S: **Maximizing solar water splitting performance by nanoscopic**

- 1 **control of the charge carrier fluxes across semiconductor–electrocatalyst junctions.** *ACS*  
2 *Catal* 2018, **8**:8545–8552.
- 3 34. Digdaya IA, Adhyaksa GWP, Trzeźniewski BJ, Garnett EC, Smith WA: **Interfacial engineering of**  
4 **metal-insulator-semiconductor junctions for efficient and stable photoelectrochemical**  
5 **water oxidation.** *Nat Commun* 2017, **8**:15968.
- 6 35. Digdaya IA, Trzeźniewski BJ, Adhyaksa GWP, Garnett EC, Smith WA: **General considerations**  
7 **for improving photovoltage in metal–insulator–semiconductor photoanodes.** *J Phys Chem C*  
8 2018, **122**:5462–5471.
- 9 36. Chen L, Yang J, Klaus S, Lee LJ, Woods-Robinson R, Ma J, Lum Y, Cooper JK, Toma FM, Wang L-  
10 W, et al.: **p-Type transparent conducting oxide/n-type semiconductor heterojunctions for**  
11 **efficient and stable solar water oxidation.** *J Am Chem Soc* 2015, **137**:9595–9603.
- 12 37. Pijpers JJH, Winkler MT, Surendranath Y, Buonassisi T, Nocera DG: **Light-induced water**  
13 **oxidation at silicon electrodes functionalized with a cobalt oxygen-evolving catalyst.** *Proc*  
14 *Natl Acad Sci USA* 2011, **108**:10056–10061.
- 15 38. Cox CR, Winkler MT, Pijpers JJH, Buonassisi T, Nocera DG: **Interfaces between water splitting**  
16 **catalysts and buried silicon junctions.** *Energy Environ Sci* 2013, **6**:532–538.
- 17 39. Sun K, Shen S, Cheung JS, Pang X, Park N, Zhou J, Hu Y, Sun Z, Noh SY, Riley CT, et al.: **Si**  
18 **photoanode protected by a metal modified ITO layer with ultrathin NiO<sub>x</sub> for solar water**  
19 **oxidation.** *Phys Chem Chem Phys* 2014, **16**:4612–4625.
- 20 40. Wang H-P, Sun K, Noh SY, Kargar A, Tsai M-L, Huang M-Y, Wang D, He J-H: **High-performance**  
21 **a-Si/c-Si heterojunction photoelectrodes for photoelectrochemical oxygen and hydrogen**  
22 **evolution.** *Nano Lett* 2015, **15**:2817–2824.
- 23 41. Benck JD, Pinaud BA, Gorlin Y, Jaramillo TF: **Substrate selection for fundamental studies of**  
24 **electrocatalysts and photoelectrodes: inert potential windows in acidic, neutral, and basic**  
25 **electrolyte.** *PLoS One* 2014, **9**:e107942.
- 26 42. Moreno-Hernandez IA, Brunschwig BS, Lewis NS: **Tin oxide as a protective heterojunction**  
27 **with silicon for efficient photoelectrochemical water oxidation in strongly acidic or alkaline**  
28 **electrolytes.** *Adv Energy Mater* 2018, **8**:1801155.
- 29 43. Mei B, Seger B, Pedersen T, Malizia M, Hansen O, Chorkendorff I, Vesborg PCK: **Protection of**  
30 **p<sup>+</sup>-n-Si photoanodes by sputter-deposited Ir/IrO<sub>x</sub> thin films.** *J Phys Chem Lett* 2014, **5**:1948–  
31 1952.
- 32 44. Jun K, Lee YS, Buonassisi T, Jacobson JM: **High photocurrent in silicon photoanodes catalyzed**  
33 **by iron oxide thin films for water oxidation.** *Angew Chemie Int Ed* 2011, **51**:423–427.
- 34 45. Strandwitz NC, Comstock DJ, Grimm RL, Nichols-Nielander AC, Elam J, Lewis NS:  
35 **Photoelectrochemical behavior of n-type Si(100) electrodes coated with thin films of**  
36 **manganese oxide grown by atomic layer deposition.** *J Phys Chem C* 2013, **117**:4931–4936.
- 37 46. Yang J, Walczak K, Anzenberg E, Toma FM, Yuan G, Beeman J, Schwartzberg A, Lin Y, Hettick  
38 M, Javey A, et al.: **Efficient and sustained photoelectrochemical water oxidation by cobalt**  
39 **oxide/silicon photoanodes with nanotextured interfaces.** *J Am Chem Soc* 2014, **136**:6191–  
40 6194.
- 41 47. Qin W, Wang N, Yao T, Wang S, Wang H, Cao Y, Liu S (Frank), Li C: **Enhancing the performance**  
42 **of amorphous-Silicon photoanodes for photoelectrocatalytic water oxidation.**  
43 *ChemSusChem* 2015, **8**:3987–3991.

- 1 48. Yang J, Cooper JK, Toma FM, Walczak KA, Favaro M, Beeman JW, Hess LH, Wang C, Zhu C, Gul  
2 S, et al.: **A multifunctional biphasic water splitting catalyst tailored for integration with high-**  
3 **performance semiconductor photoanodes.** *Nat Mater* 2016, **16**:335.
- 4 49. Zhou X, Liu R, Sun K, Papadantonakis KM, Brunschwig BS, Lewis NS: **570 mV photovoltage,**  
5 **stabilized n-Si/CoO<sub>x</sub> heterojunction photoanodes fabricated using atomic layer deposition.**  
6 *Energy Environ Sci* 2016, **9**:892–897.
- 7 50. Sun K, McDowell MT, Nielander AC, Hu S, Shaner MR, Yang F, Brunschwig BS, Lewis NS: **Stable**  
8 **solar-driven water oxidation to O<sub>2</sub>(g) by Ni-oxide-coated silicon photoanodes.** *J Phys Chem*  
9 *Lett* 2015, **6**:592–598.
- 10 51. Zhou X, Liu R, Sun K, Friedrich D, McDowell MT, Yang F, Omelchenko ST, Saadi FH, Nielander  
11 AC, Yalamanchili S, et al.: **Interface engineering of the photoelectrochemical performance of**  
12 **Ni-oxide-coated n-Si photoanodes by atomic-layer deposition of ultrathin films of cobalt**  
13 **oxide.** *Energy Environ Sci* 2015, **8**:2644–2649.
- 14 52. Sun K, Saadi FH, Lichterman MF, Hale WG, Wang H-P, Zhou X, Plymale NT, Omelchenko ST, He  
15 J-H, Papadantonakis KM, et al.: **Stable solar-driven oxidation of water by semiconducting**  
16 **photoanodes protected by transparent catalytic nickel oxide films.** *Proc Natl Acad Sci USA*  
17 2015, **112**:3612–3617.
- 18 53. Mei B, Permyakova AA, Frydendal R, Bae D, Pedersen T, Malacrida P, Hansen O, Stephens IEL,  
19 Vesborg PCK, Seger B, et al.: **Iron-treated NiO as a highly transparent p-type protection layer**  
20 **for efficient Si-based photoanodes.** *J Phys Chem Lett* 2014, **5**:3456–3461.
- 21 54. Bae D, Mei B, Frydendal R, Pedersen T, Seger B, Hansen O, Vesborg PCK, Chorkendorff I: **Back-**  
22 **illuminated Si-based photoanode with nickel cobalt oxide catalytic protection layer.**  
23 *ChemElectroChem* 2016, **3**:1546–1552.
- 24 55. Kenney MJ, Gong M, Li Y, Wu JZ, Feng J, Lanza M, Dai H: **High-performance silicon**  
25 **photoanodes passivated with ultrathin nickel films for water oxidation.** *Science* 2013,  
26 **342**:836–840.
- 27 56. Han T, Shi Y, Song X, Mio A, Valenti L, Hui F, Privitera S, Lombardo S, Lanza M: **Ageing**  
28 **mechanisms of highly active and stable nickel-coated silicon photoanodes for water**  
29 **splitting.** *J Mater Chem A* 2016, **4**:8053–8060.
- 30 57. Li S, She G, Chen C, Zhang S, Mu L, Guo X, Shi W: **Enhancing the photovoltage of Ni/n-Si**  
31 **photoanode for water oxidation through a rapid thermal process.** *ACS Appl Mater Interfaces*  
32 2018, **10**:8594–8598.
- 33 58. Laskowski FAL, Nellist MR, Venkatkarthick R, Boettcher SW: **Junction behavior of n-Si**  
34 **photoanodes protected by thin Ni elucidated from dual working electrode**  
35 **photoelectrochemistry.** *Energy Environ Sci* 2017, **10**:570–579.
- 36 59. Sun K, Ritzert NL, John J, Tan H, Hale W, Jiang J, Moreno-Hernandez IA, Papadantonakis KM,  
37 Moffat TP, Brunschwig BS, et al.: **Performance and failure modes of Si anodes patterned with**  
38 **thin-film Ni catalyst islands for water oxidation.** *Sustain Energy Fuels* 2018, **2**:983–998.
- 39 60. Oh S, Oh J: **High performance and stability of micropatterned oxide-passivated photoanodes**  
40 **with local catalysts for photoelectrochemical water splitting.** *J Phys Chem C* 2016, **120**:133–  
41 141.
- 42 61. Oh S, Song H, Oh J: **An optically and electrochemically decoupled monolithic**  
43 **photoelectrochemical cell for high-performance solar-driven water splitting.** *Nano Lett* 2017,  
44 **17**:5416–5422.

- 1 62. Ji L, Hsu HY, Li X, Huang K, Zhang Y, Lee JC, Bard AJ, Yu ET: **Localized dielectric breakdown and**  
2 **antireflection coating in metal-oxide-semiconductor photoelectrodes.** *Nat Mater* 2017,  
3 **16:127–131.**
- 4 63. Sun K, Park N, Sun Z, Zhou J, Wang J, Pang X, Shen S, Noh SY, Jing Y, Jin S, et al.: **Nickel oxide**  
5 **functionalized silicon for efficient photo-oxidation of water.** *Energy Environ Sci* 2012,  
6 **5:7872–7877.**
- 7 64. Contractor AQ, Bockris JOM: **Investigation of a protective conducting silica film on n-silicon.**  
8 *Electrochim Acta* 1984, **39:1427–1434.**
- 9 65. Yu X, Yang P, Chen S, Zhang M, Shi G: **NiFe alloy protected silicon photoanode for efficient**  
10 **water splitting.** *Adv Energy Mater* 2017, **7:1–6.**
- 11 66. Dong WJ, Song YJ, Yoon H, Jung GH, Kim K, Kim S, Lee J-L: **Monolithic photoassisted water**  
12 **splitting device using anodized Ni-Fe oxygen evolution catalytic substrate.** *Adv Energy Mater*  
13 2017, **7:1700659.**
- 14 67. Tung RT: **The physics and chemistry of the Schottky barrier height.** *App Phys Rev* 2014,  
15 **011304.**
- 16 68. Ohdomari I, Aochi H: **Size effect of parallel silicide contact.** *Phys Rev B* 1987, **35:682–686.**
- 17 69. Freeouf JL, Jackson TN, Laux SE, Woodall JM: **Size dependence of "effective" barrier heights**  
18 **of mixed-phase contacts.** *J Vac Sci Technol* 1982, **21:570–573.**
- 19 70. Tung RT: **Electron transport of inhomogeneous Schottky barriers.** *Appl Phys Lett* 1991,  
20 **58:2821–2823.**
- 21 71. Yae S, Tsuda R, Kai T, Kikuchi K, Uetsuji M, Fujii T, Fujitani M, Nakato Y: **Efficient**  
22 **photoelectrochemical solar cells equipped with an n-Si electrode modified with colloidal**  
23 **platinum particles.** *J Electrochem Soc* 1994, **141:3090–3095.**
- 24 72. Nakato Y, Tsubomura H: **Silicon photoelectrodes modified with ultrafine metal islands.**  
25 *Electrochim Acta* 1992, **37:897–907.**
- 26 73. Rossi RC, Lewis NS: **Investigation of the size-scaling behavior of spatially nonuniform barrier**  
27 **height contacts to semiconductor surfaces using ordered nanometer-scale nickel arrays on**  
28 **silicon electrodes.** *J Phys Chem B* 2001, **105:12303–12318.**
- 29 74. Fabre B: **Functionalization of oxide-free silicon surfaces with redox-active assemblies.** *Chem*  
30 *Rev* 2016, **116:4808–4849.**
- 31 75. Hill JC, Landers AT, Switzer JA: **An electrodeposited inhomogeneous metal–insulator–**  
32 **semiconductor junction for efficient photoelectrochemical water oxidation.** *Nat Mater* 2015,  
33 **14:1150–1155.**
- 34 76. Loget G, Fabre B, Fryars S, Mériadec C, Ababou-Girard S: **Dispersed Ni nanoparticles stabilize**  
35 **silicon photoanodes for efficient and inexpensive sunlight-assisted water oxidation.** *ACS*  
36 *Energy Lett* 2017, **2:569–573.**
- 37 77. Oh K, Mériadec C, Lassalle-Kaiser B, Dorcet V, Fabre B, Ababou-Girard S, Joanny L,  
38 Gouttefangeas F, Loget G: **Elucidating the performance and unexpected stability of partially**  
39 **coated water-splitting silicon photoanodes.** *Energy Environ Sci* 2018, **11:2590–2599.**
- 40 78. Lee SA, Lee TH, Kim C, Lee MG, Choi M-J, Park H, Choi S, Oh J, Jang HW: **Tailored NiO<sub>x</sub>/Ni**  
41 **cocatalysts on silicon for highly efficient water splitting photoanodes via pulsed**  
42 **electrodeposition.** *ACS Catal* 2018, **8:7261–7269.**

- 1 79. Xu G, Xu Z, Shi Z, Pei L, Yan S, Gu Z, Zou Z: **Silicon photoanodes partially covered by**  
2 **Ni@Ni(OH)<sub>2</sub> core–shell particles for photoelectrochemical water oxidation.** *ChemSusChem*  
3 2017, **10**:2897–2903.
- 4 80. Stevens MB, Enman LJ, Batchellor AS, Cosby MR, Vise AE, Trang CDM, Boettcher SW:  
5 **Measurement techniques for the study of thin film heterogeneous water oxidation**  
6 **electrocatalysts.** *Chem Mater* 2017, **29**:120–140.
- 7 81. Tung CW, Chuang Y, Chen HC, Chan TS, Li JY, Chen HM: **Tunable electrodeposition of Ni**  
8 **electrocatalysts onto Si microwires array for photoelectrochemical water oxidation.** *Part*  
9 *Part Syst Charact* 2018, **35**:1700321.
- 10 82. Kasemthaveechok S, Oh K, Fabre B, Bergamini J-F, Mériadec C, Ababou-Girard S, Loget G: **A**  
11 **general concept for solar water-splitting monolithic photoelectrochemical cells based on**  
12 **earth-abundant materials and a low-cost photovoltaic panel.** *Adv Sustain Syst* 2018,  
13 **2**:1800075.
- 14 83. Zhao J, Gill TM, Zheng X: **Enabling silicon photoanodes for efficient solar water splitting by**  
15 **electroless-deposited nickel.** *Nano Res* 2018, **11**:3499–3508.
- 16 84. Chen J, Xu G, Wang C, Zhu K, Wang H, Yan S, Yu Z, Zou Z: **High-performance and stable silicon**  
17 **photoanode modified by crystalline Ni@ amorphous Co core-shell nanoparticles.**  
18 *ChemCatChem* 2018, **10**:5025.
- 19